



## PROPOSAL OF AN EFFICIENT TECHNIQUE FOR RETROFITTING UNREINFORCED MASONRY DWELLINGS

Paola MAYORCA<sup>1</sup> and Kimiro MEGURO<sup>2</sup>

### SUMMARY

Masonry structures are widely used due to its low cost and construction easiness especially in developing countries. In spite of the efforts to provide guidelines for the construction of sound earthquake resistant houses, every year casualties due to collapsing masonry houses during earthquakes are reported. Although it is clear that retrofitting the existing housing stock is urgent, successful campaigns oriented in this direction are scarce or inexistent. To overcome this situation, retrofitting techniques involving inexpensive construction materials available in remote regions and low-skill labor as well as aggressive educational campaigns are needed. This paper presents an innovative retrofitting method for masonry houses, which consists of using polypropylene bands arranged in a mesh fashion and embedded in a mortar overlay. These bands, which are commonly used for packing, are resistant, inexpensive, durable and worldwide available. In order to verify the suitability of the proposed method, a series of masonry walls, with and without retrofit, were tested under in-plane loads. Although the retrofitted wall peak strength was almost the same as that of the bare wall, its post-peak strength was larger and sustained for lateral drifts over 2%. In order to investigate the proposed retrofitting features for different material properties and mesh configurations, numerical simulations based on a discrete modeling approach were performed. The effects of the band mesh pitch and connection distribution combined with different masonry types were examined.

### INTRODUCTION

Masonry is a construction material widely used around the world due to its low cost and construction easiness. More than 30% of the world's population lives in a house of unbaked earth, which is one type of unreinforced masonry [1]. During the last century, human casualties during earthquakes were mainly caused by structural damage, being the failure of unreinforced masonry structures responsible of more than 60% of them [2]. The vulnerability of masonry structures under seismic loads has being recognized long ago and efforts to provide guidelines for the construction of sound earthquake resistant houses have

---

<sup>1</sup> Post-doctoral fellow, Institute of Industrial Science, University of Tokyo, Japan. Email: [paola@iis.u-tokyo.ac.jp](mailto:paola@iis.u-tokyo.ac.jp)

<sup>2</sup> Associate Professor, ditto. Email: [meguro@iis.u-tokyo.ac.jp](mailto:meguro@iis.u-tokyo.ac.jp)

being remarkable. In spite of this, every year many casualties due to collapsing masonry houses during earthquakes are reported.

Several types of retrofitting methods have been developed for unreinforced masonry structures. A comprehensive review of them can be found in Lizundia et al [3]. The existing retrofitting techniques can be categorized in: 1) grout and epoxy injections, 2) surface coatings, 3) reinforced or post-tensioned cores, and 4) addition of structural elements. There is no doubt that these methods are useful for strengthening masonry structures. Depending on the purpose of the retrofitting works, one method is more appealing than the other.

For strengthening unreinforced masonry houses in developing countries, a suitable retrofitting technique should guarantee not only its efficiency in terms of improvement of the seismic resistant characteristics of the structure (strength, ductility and energy dissipation). It should also be considered that: 1) the used material is economical and locally available and 2) the required labor skill is minimum. In this context, a new retrofitting method for unreinforced masonry structures is proposed.

### **RETROFITTING METHOD PROPOSAL**

The proposed retrofitting method is based on polypropylene bands (PP-bands) arranged in a mesh fashion and embedded in a cement mortar overlay. These bands, which are worldwide used for packing, are inexpensive, resistant, and easy to handle. The retrofitting installation procedure is as follows:

1. The PP-bands are arranged in a mesh fashion and connected at their crossing points (Figure 1).
2. At the mesh borders, which coincide with the wall top and bottom, two steel rods are installed as shown in Figure 2. Because it is difficult to paste the PP-band with other material such as brick or concrete, these bars are used to anchor the mesh at the foundation and wall top edge.
3. The walls are cleaned and if possible the paint is removed. Any loose brick pieces are removed and replaced.
4. 6mm-diameter holes are drilled through the wall at approximately 250 to 300mm pitch. If the masonry units are relatively strong, it is preferable to place the holes at the weak mortar interface. The drilled holes are cleaned with water spray or air.
5. The meshes are installed on both sides of the wall and wrapped around the corners and wall edges. An overlapping length of approximately 300mm is needed.
6. Wire is passed through the previously drilled wall holes and used to connect the meshes on both wall sides. In order to prevent the wires from cutting the PP-band mesh, a plastic piece or any other stiff element is placed between the band and the wire. It is desirable to have connectors close to the wall intersections and wall edges.
7. The top/bottom mesh edges, where steel bars are installed, are pasted to the foundation and wall top border utilizing epoxy. The epoxy is used to connect the bars and the wall and it is not directly applied to the mesh. The bands, which are rolled around the bars, transfer their load through friction. Epoxy is a relatively costly material and would increase the construction cost. Therefore other options to anchor the mesh are been considered. For instance, it is possible to cut a groove on the bottom and top of the wall, install inside it the anchoring bars, and finally seal it with cement mortar. This arrangement, however, has not been tested yet.
8. The mesh overlapping lengths are pasted to the adjacent wall meshes. In this way, the reinforcement system continuity is enhanced. This step concludes the setting of the PP-band mesh (Figure 3).
9. In order to protect the mesh from the Ultra Violet radiation, rain, and eventually vandalism, a mortar layer is placed on the retrofitted wall. Before the mortar is applied, the wall is wetted. The mortar overlay is expected to provide not only protection but also anchoring to the PP-band mesh.



Figure 1. PP-band mesh



Figure 2. Detail of the top/bottom connection



Figure 3. Retrofitted wall before mortar overlay setting

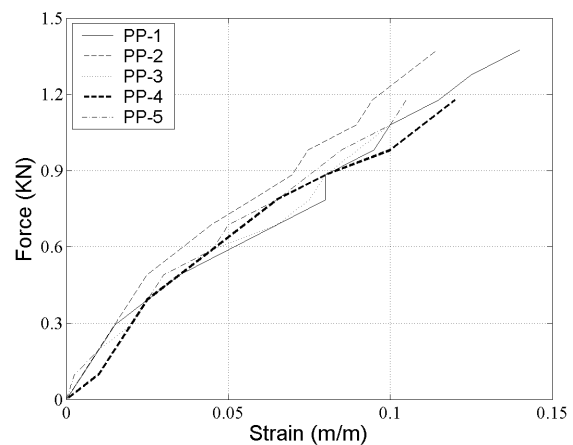


Figure 4. Force-strain relation of one PP-band

## EXPERIMENTAL PROGRAM

In order to assess the suitability of using PP-band meshes for retrofitting masonry walls, an experimental program, consisting of material and shear wall testing, was carried out. Clay bricks and cement mortar were used in the program. The mortar mix proportion, in volume, was cement:sand=1:4.5 and the joint thickness was 10mm.

### Material testing

Cement mortar, clay brick, and masonry properties were determined. Five specimens were prepared for each test. The masonry specimens were cured with water spray for 14 days during which they were covered with plastic sheets. The results of these tests are summarized in Table 1.

The PP-band properties were also investigated through direct tension tests of five samples (PP-1 through PP-5). The obtained force-strain graphs are shown in Figure 4. Three out of five bands failed before reaching 1.2kN, which is the nominal band strength. All of them, however, exhibited a large deformation capability, more than 10% strain in all of the cases. The force-strain curve is fairly bilinear with an initial and residual stiffness of 16.5 and 8.9 KN×m/m, respectively. Given the relatively low stiffness of the PP-band, it was not expected that it would contribute to increase the masonry wall strength. However, given its large deformation capacity, it could improve the structure ductility.

**Table 1. Material properties**

Material	Property	Value
Brick	Compression strength, $f_{cb}$ (MPa)	80.0
	Young's Modulus, $E_b$ (GPa)	15.7
	Splitting tensile strength, $f_{tb}$ (MPa)	4.2
	Poisson's ratio, $\nu_b$	0.14
Mortar	Compression strength, $f_{cj}$ (MPa)	8.2
	Tensile strength, $f_{tb}$ (MPa)	0.7
	Young's Modulus, $E_j$ (GPa)	8.6
	Poisson's ratio, $\nu_j$	0.2
Masonry	Compression strength, $f_{cm}$ (MPa)	36.9
	Bond strength, $f_{tm}$ (MPa)	1.05
	Cohesion strength, $c$ (MPa)	1.13

**Shear wall testing**

Eight masonry walls were constructed: four with and four without reinforcement. The wall dimensions were 985mm×1072mm×100mm and consisted of 15 brick rows of 4.5 bricks each. The bottom and top brick layers were embedded in steel channels. The bottom channel was welded to a steel plate, which was used to bolt the specimen to the loading frame. In order to prevent the wall sliding, two stoppers at the wall toes were provided. At the end of the curing process, which was the same as the one for the material test specimens, the upper channel was installed. Figure 5 shows the test setup and the sign convention of the measured loads and displacements.

Two meshes, as shown in Figure 1, were prepared per retrofitted wall. The mesh pitch, equal to 45mm, was chosen so that each brick would be crossed by at least three bands. The connectors, 27 in total, were placed only at the mortar interface. This constrain defined the band inclination, which was 50°. A cement mortar mix (cement:sand=1:3) was used for the protection overlay of 8mm thickness.

At first, a vertical pre-compression load was applied by closing the bolts at the bottom end of six vertical rods while monitoring the force increment. Then, the actuator was positioned and the forces at the vertical rods were readjusted in case of unbalance. Finally, the horizontal loading, which consisted of 5 steps was applied with a hydraulic pump operated manually. In the first step, the wall was loaded until diagonal cracking. The second step consisted on additionally pushing the wall 10mm in the same direction. In the third step, the actuator displacement direction was reversed and the specimen was loaded until the diagonal crack in the opposite direction occurred. In the fourth step, the wall was loaded 10mm more in the same direction. Finally, the wall was unloaded. Table 2 shows the experiment program summary.

**Table 2. Summary of experiment conditions**

Case name	VL (kN)	PP-band	Mortar	Holes
Bare wall	9			None
Bare wall w/holes	9			Uniform
Bare wall w/mortar	9		O	None
Reinforced wall	9	O	O	None
Reinforced wall w/holes	9	O	O	Uniform
Bare wall w/mortar	30		O	None
Reinforced wall	30	O	O	None
Reinforced wall w/diagonal holes	30	O	O	Diagonal

VL: Vertical pre-compression load

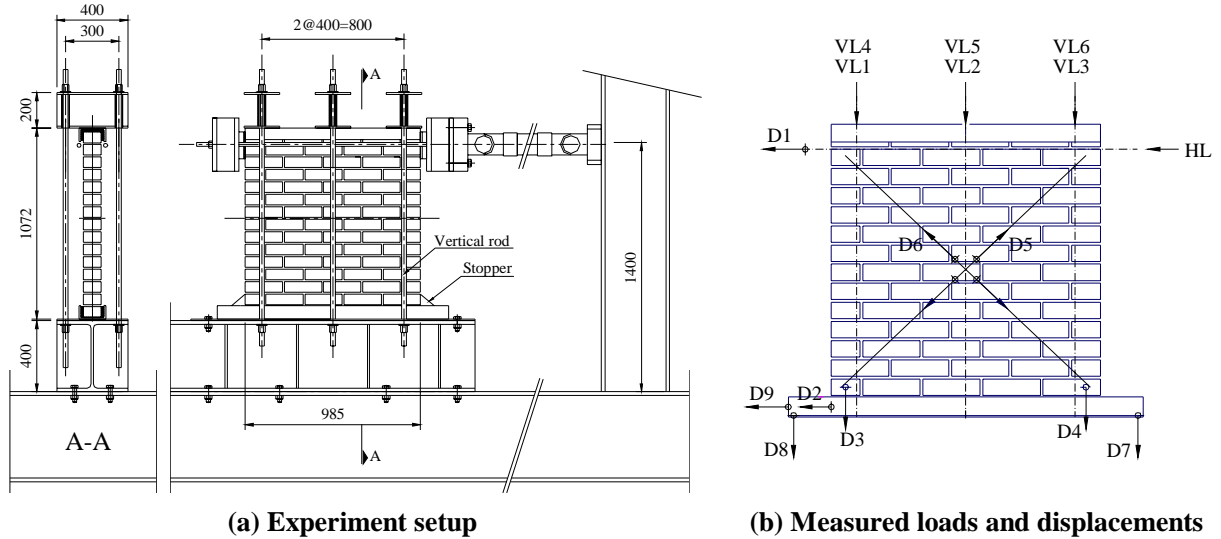


**Figure 5. Experiment setup and measured loads (VL and HL) and displacements (D1 through D9)**

Due to the high brick strength, the resulting masonry was stronger than the material typically available in developing countries. In order to intentionally reduce the wall strength and highlight the retrofitting effect, holes were drilled through some of the walls. Two hole distributions were considered, uniform and diagonal. Further details of the experimental program may be found in Mayorca [4].

## RESULTS DISCUSSION

The experimental observations are briefly discussed below.

### Crack pattern

As observed in Figures 6 and 7, the crack location is similar for both unreinforced and reinforced walls. In both cases, the bending tensile stresses caused a crack at the lower most mortar layer at an early load stage. This crack became gradually longer and wider as the horizontal load increased. In the walls with VL=9kN, the bottom crack was accompanied by a strength drop. This, however, was small in the case of the reinforced walls because the mesh limited the crack propagation and opening.

The flexural crack caused the horizontal force, which was originally transferred to the support by a shear-flexural mechanism, to be resisted through a compression strut along the wall diagonal. As the bottom crack stopped propagating, the specimen stresses continued to build up and were eventually released through a diagonal crack. In the unreinforced masonry wall, a single crack was observed while in the reinforced masonry case, the crack was distributed along a wider band.

After the first diagonal crack, the wall strength was notoriously reduced and the subsequent imposed deformation was related to the movement of the upper portion of the cracked wall. Because of this, when the load was reversed, it did not produce any additional flexural cracking. It was mainly the upper wall displacement. After the initial shear crack closed, the stresses started to build up again and the second diagonal crack, along the other diagonal, appeared. In this case again, the reinforced wall cracks were distributed along a wide zone as opposed to the unreinforced wall crack which was concentrated.



### **Stiffness**

The force-displacement curves presented in Figure 8 may suggest that, after the bending tensile crack, the reinforced walls have a slightly higher stiffness than the unreinforced ones. However, it must be noted that the showed displacements correspond to two effects, the wall deformation itself and the wall rotation. The later is dominant. Figure 10 depicts the deformation along the wall diagonals, which directly reflects the wall shear deformation. In this case the reinforced and unreinforced wall deformations are small and almost the same. This shows the high shear stiffness of the masonry wall and confirms that the stiffness difference observed in the force deformation curves is mainly due to the PP-band mesh restraint to the wall rotation.

### **Peak strength**

The PP-bands have a relatively low stiffness compared to the masonry walls [4]. Because of this, they did not contribute to increase the wall peak strength. Although some differences are observed, these are due to: 1) mortar overlay, 2) bonding between mortar overlay and masonry wall, and 3) variability of masonry properties due to the workmanship effect. The PP-band mesh contribution is only appreciated after the wall diagonally cracked.

### **Post-peak strength**

Figure 11 shows the force-displacement relation normalized to the peak strength and corresponding displacement for the group of walls with  $V_L=9\text{kN}$ . It is observed that immediately after the peak, the normalized strength dropped to 10 to 40% for the unreinforced walls. On the other hand, the reinforced walls exhibited a 60% residual strength after the peak, which was sustained for deformations equivalent to almost three times the deformation at which the diagonal crack occurred, .i.e. at least 2% lateral drift. In the reverse direction, the reinforced walls also exhibited larger normalized strength.

### **Effect of connectors and mortar overlay**

The reinforced wall with  $V_L=30\text{kN}$  deserves special attention because the wall strength after the diagonal crack dropped to almost 25% of the peak strength. This was the only reinforced wall that exhibited such a sharp drop. After the test, the specimen was examined and broken wire connectors were found. Furthermore, a severe cracking of the mortar overlay due to drying shrinkage was observed before the experiment. This may have caused a reduction of the mortar support to the bands resulting in a larger demand to the wire connections, which ultimately caused their failure. It is worth noting that this was the first retrofitted wall constructed and due to the lack of experience in the installation process, the steel wires were occasionally damaged during the mesh setting.

## **NUMERICAL SIMULATIONS**

The experiments described in the previous section showed the effects of retrofitting masonry walls with PP-band meshes. These results, however, can only be discussed for a limited range of masonry and mesh properties. In order to broaden the discussion, different masonry types and mesh configurations should be considered. In order to do this, numerical simulations are used.

The numerical analysis was carried out with the Applied Element Method (AEM), an analysis technique based on a discrete model approach. With the AEM a structure can be analyzed from early stages of loading until large material and geometrical nonlinearities occur. In the AEM, the structure is virtually divided in elements connected through couples of normal and shear springs. Mass and damping properties are lumped at the elements and the springs have normal and shear stiffness. Complex cracking patterns can be followed without predefinition of crack locations. The details of the AEM general formulation may be found in Tagel-Din H. and Meguro [5] and those directly related to masonry and mesh modeling in Mayorca [4].

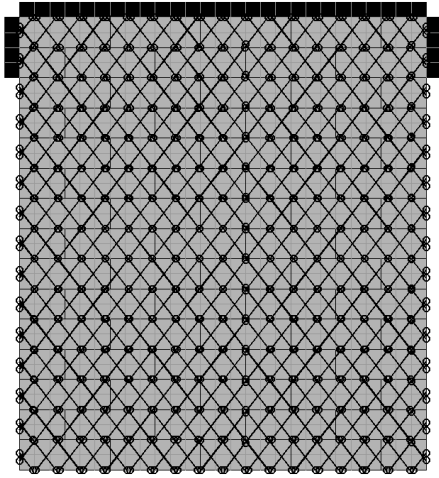


Figure 12. Reinforced masonry wall model

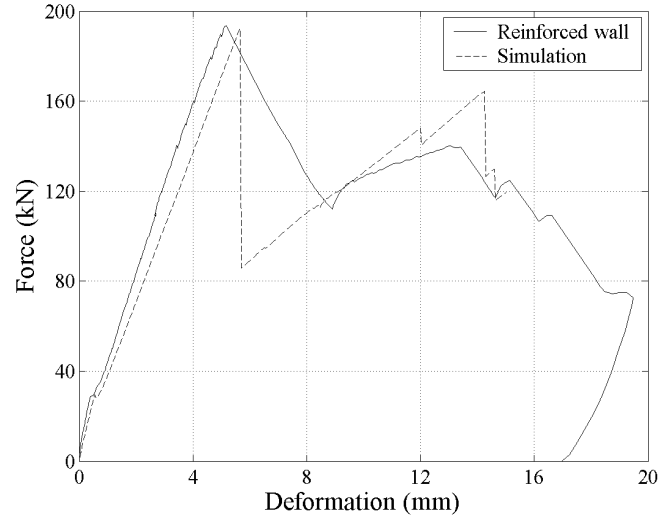


Figure 13. Experimental and simulated force-deformation relation

At first, the model is validated by comparing the analysis results with the experimental observation. After this, a parametric study considering different masonry properties, mesh distribution and connector location is carried out and the results discussed.

### Model validation

The structure was idealized as shown in Figure 12. Each brick consisted of  $6 \times 2$  elements and five springs/element side were considered. The loading plates and I-beams on top of the wall were modeled with steel elements. The latter served as connection points for the vertical steel rods. The bottom brick layer was considered fixed and the stopper was simulated by restraining the horizontal displacement of the two brick elements adjacent to the stopper. The vertical preloading (load control) was applied to the steel plates on top of the wall after which the horizontal deformation was prescribed on the steel elements at the upper wall corner (displacement control). The material properties used for the analysis are shown in Table 3. These are the values obtained in the material testing program supplemented from values obtained from the literature [6, 7]. The mesh band parameters are summarized in Table 4..

Table 3. Masonry properties used for the analysis

$E_b$ (GPa)	$E_j$ (GPa)	$f_{tm}$ (MPa)	$c$ (MPa)	$G_f^I$	$G_f^{II}$	$\tan\phi$	$f_{cb}$ (MPa)	$f_{tb}$ (MPa)
				$(\times 10^{-3} \text{ kN} \times \text{mm} / \text{mm}^2)$				
15.7	0.34	1.05	2.30	0.068	0.199	0.8	80.0	4.2

$G_f^I$ : Mode I fracture energy

$G_f^{II}$ : Mode II fracture energy

$\phi$ : Mortar interface friction angle

Table 4. PP-band properties used in the analysis

$F_y$ (kN)	$F_u$ (kN)	$E_o$ (kN×m/m)	$E_r$ (kN×m/m)
0.50	1.35	16.5	8.9

$F_y$ : Yielding strength

$F_u$ : Ultimate strength

$E_o$ : Initial stiffness

$E_r$ : Residual stiffness

The modulus of elasticity of the mortar used in the analysis is different from the one obtained in the material testing. The mortar conditions at the masonry wall joint and at the specimen used in the material test, a cylinder in the present case, are different. Therefore, it is not accurate to directly apply the parameter obtained in the mortar compression test to the simulation. For the present analysis, the mortar modulus of elasticity was determined so that the initial slopes of the simulated and observed force-deformation curves coincide.

The experimental program showed the importance of the mortar overlay and mesh connectors in the performance of the strengthened walls and thus, they should be included in the numerical model. However, for this purpose it is necessary to determine the mortar-wall and mortar-mesh bonding characteristics. The data obtained during the experimental program is insufficient to include these effects directly. Therefore, they were considered indirectly by: 1) increasing the cohesion strength, and 2) considering a larger number of connectors between the mesh and wall (as shown in Figure 12, in which the circles represent the connector locations.)

Figure 13 shows the comparison between the experimental results and the simulation. The model captured the main features of the behavior, i.e. flexural and diagonal cracking and consequent strength drop. The observed stiffness after the initiation of the nonlinear behavior, i.e. flexural crack appearance, is larger than the simulated stiffness. This is related to the bottom flexural crack propagation and opening. In the experiments, the crack at this location has a width of approximately 1 to 2 mm. If the mortar overlay effectively connected the PP-band mesh and the wall, the free band length is the same as the mortar crack width, i.e. 1 to 2 mm. The connectors considered in the model do not reflect this situation. In the model, the free band length is approximately 80mm, resulting in a more flexible element. The small band stiffness at the bottom crack may be the reason why the PP-band effect on the bottom crack propagation and wall rotation was underestimated.

After the diagonal cracking occurs, a sharp strength drop is observed. Due to the limitations of the recording system, there is no experimental data registering the crack occurrence process. However, if the measured points just before and after the crack appearance are compared with the numerical simulation curve, a fair agreement is observed. During the experiments, the wall strength slightly increased after the strength drop associated with the diagonal crack. In the simulation this effect was observed, although the strength increase rate was larger.

Figure 14 shows the deformed shapes of unreinforced and reinforced walls at 5, 10 and 15mm deformation. In the unreinforced case it is clear that the upper portion of the wall freely slid after the diagonal crack occurred. On the other hand, in the reinforced wall, the bricks on the bottom corner of the upper wall portion stuck to the lower portion and rotated. This increased the friction resistance and the strength increment rate observed after the peak. The deformed shapes also show that the diagonal crack, which was concentrated in the case of the unreinforced wall, was distributed over a wider area in the case of the reinforced wall.

Figure 15 shows the distribution of vertical normal stresses in the wall. In both cases, the distribution is very similar before the diagonal cracking. However, after its occurrence there is a redefinition of the load transfer paths. In the case of the unreinforced wall, basically one path is observed whereas in the reinforced wall two paths on both sides of the crack are distinguished. Although the peak strength of the wall is not improved by the reinforcement, the stress state inside the wall after the diagonal crack is considerably affected and consequently a larger post-peak strength is observed for the reinforced walls.

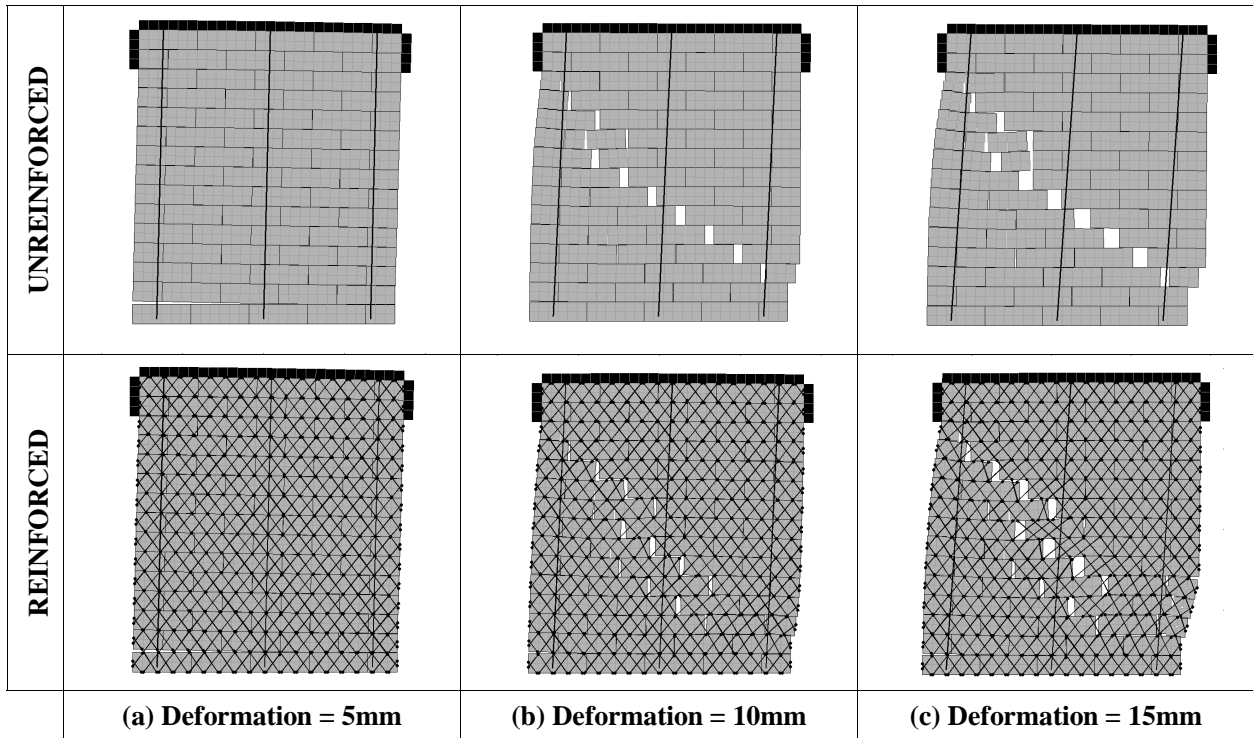


Figure 14. Deformed shapes for unreinforced and reinforced walls (Scale factor=5)

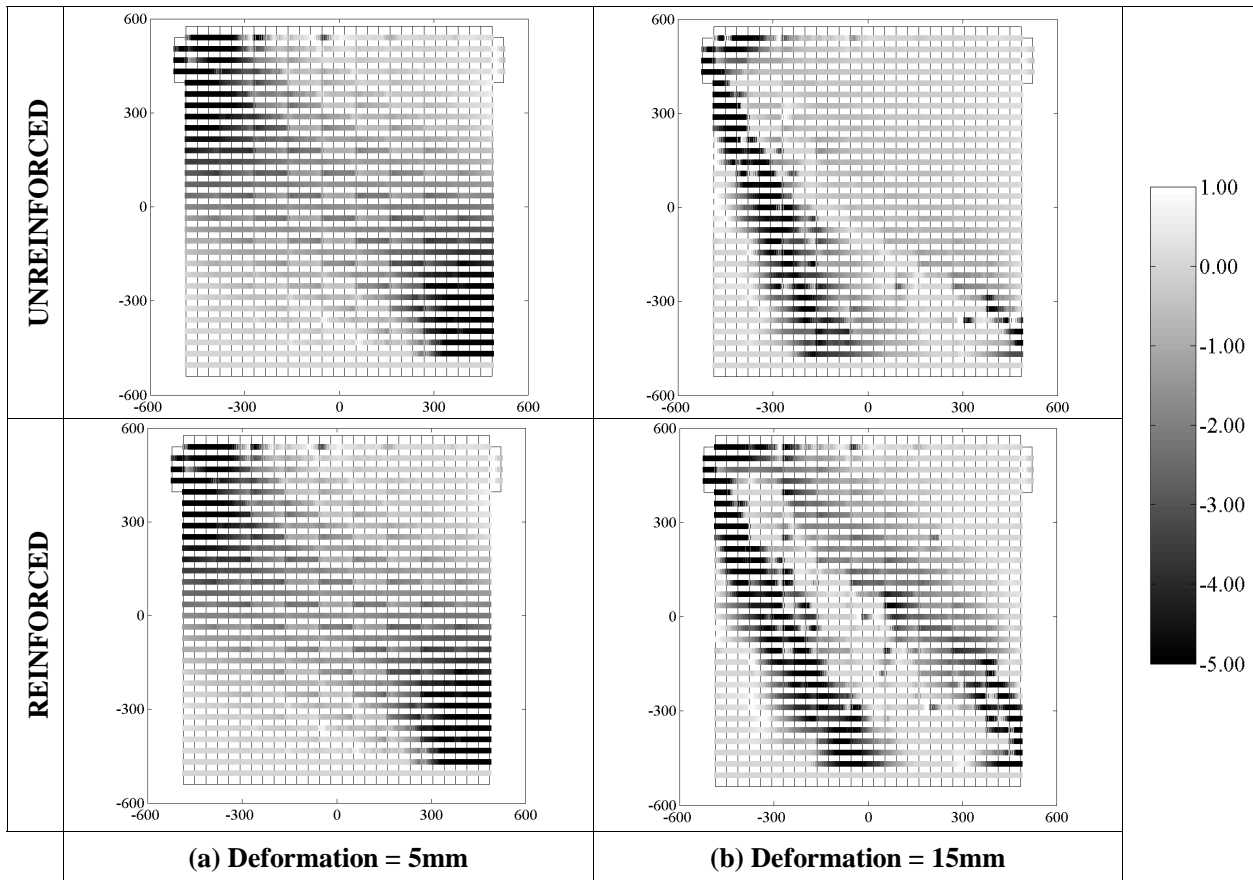


Figure 15. Vertical normal stress distribution in unreinforced and reinforced walls (in MPa)

### Parametric study

In order to investigate the effects of different reinforcement patterns on various masonry types, a parametric study of reinforced walls was carried out. The parameters that were examined are shown in Table 5. In all the cases a vertical pre-compression load equal to 9kN was considered.

**Table 5. Parameters considered in the parametric study of reinforced walls**

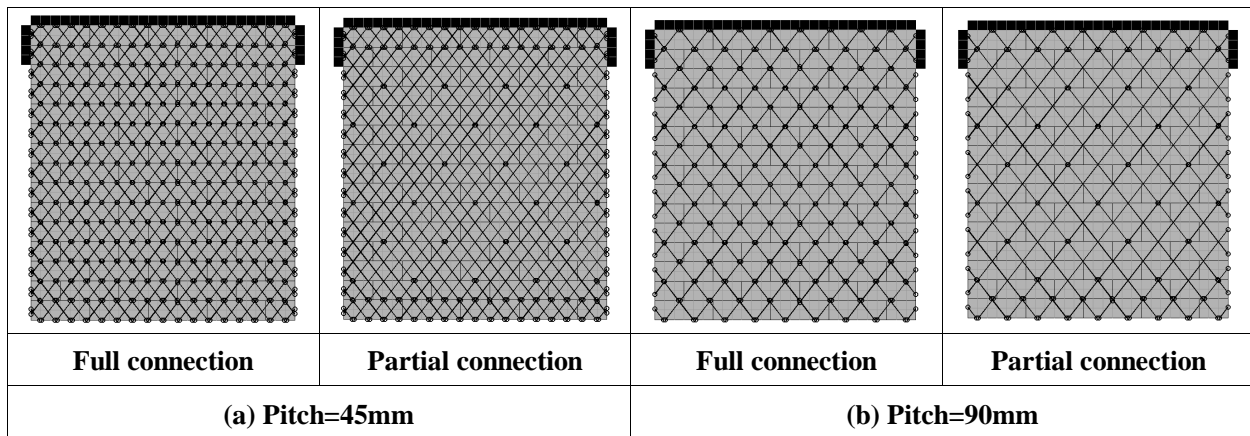
Parameter	Remarks
Mesh pitch	45 and 90mm
Connection level	Full and partial
Wall type	Strong and weak

The evaluation of the mesh pitch and connection level effect on the behavior of the reinforced walls was considered necessary to assess which is more relevant to the retrofitted structure performance. The different combinations are shown in Figure 16.

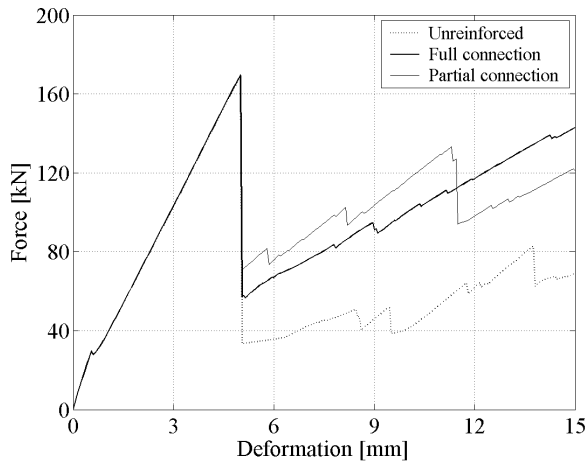
The relation between the wall and reinforcement strengths and stiffness may also affect the reinforced wall behavior. Given the wide variety of masonry available in the world, especially weaker structures in developing countries, it is reasonable to investigate the variation of the failure mechanism when the reinforcement is applied to such weak materials. The properties of weak masonry, which are available in the literature [8], indicate that masonry with strengths equal to 10% of the strength of the walls used in the experiments is not unusual. For the present parametric study, the weak wall properties were defined as equal to 10% of the values obtained in the material tests presented in Table 3. Because it would be unrealistic to reduce the friction coefficient by a factor of 10, this parameter was reduced by only 25%.

Figure 17 shows the force-deformation relations for the strong wall cases. Although the peak strengths are the same, the residual strengths after the diagonal crack are larger for the reinforced walls. The mesh pitch and connection level influence the residual strength. Larger pitches and fewer connectors reduced the reinforcement beneficial effects. A 90-mm pitch mesh fully connected may perform as well as a 45-mm pitch mesh with fewer connectors.

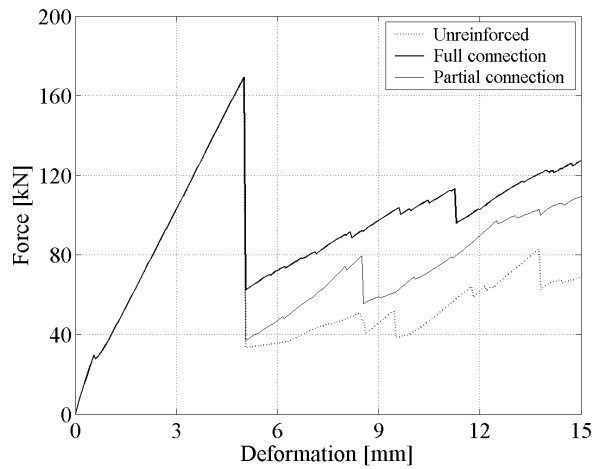
Figure 18 presents the force deformation curves for the reinforced weak walls. Again the post-peak strength is larger in the reinforced wall case. Although the mesh pitch has a strong influence in the behavior, the connection level effect is not so evident, especially for the 90-mm pitch mesh. As opposed to the strong wall case, in this case, a well anchored 90-mm pitch did not perform as well as a partially anchored 45-mm pitch mesh.



**Figure 16. Mesh pitch and connection level considered for the parametric study**

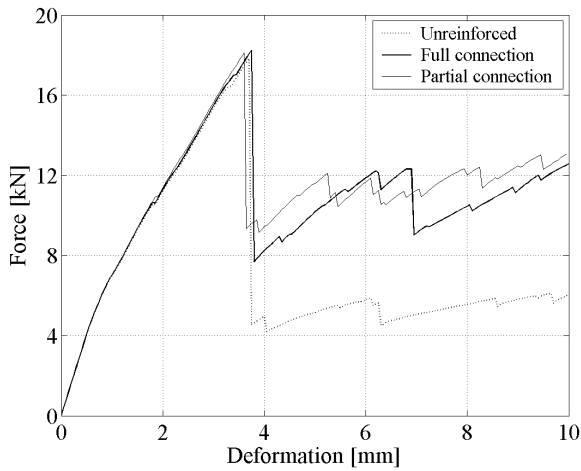


(a) Pitch=45mm

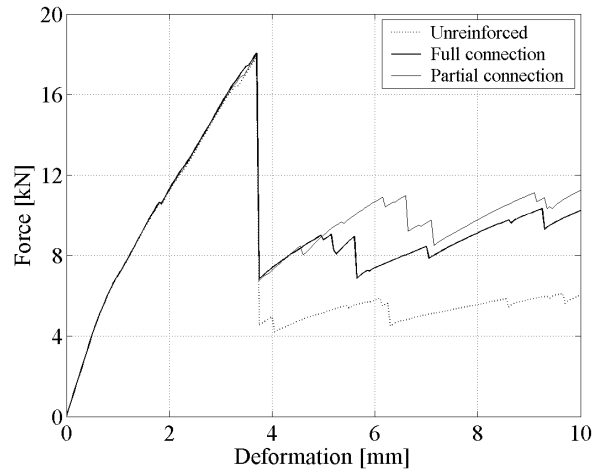


(b) Pitch=90mm

Figure 17. Force-deformation curve for reinforced wall (Strong walls)

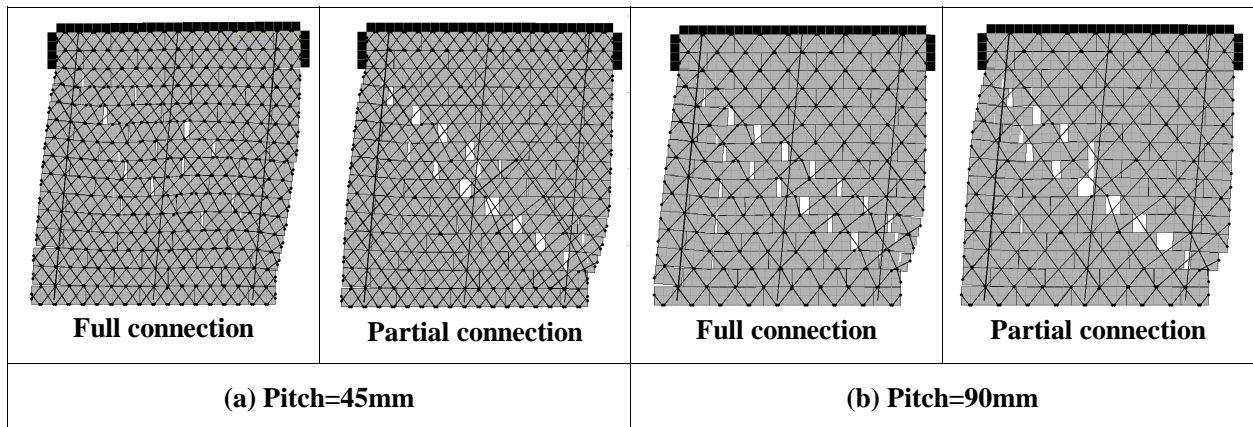


(a) Pitch=45mm



(b) Pitch=90mm

Figure 18. Force-deformation curve for reinforced wall (Weak walls)



(a) Pitch=45mm

(b) Pitch=90mm

Figure 19. Deformed shapes of weak walls reinforced with PP-band mesh – Deformation = 10mm (Scale factor = 5)

The relation between the strength immediately after and before the shear crack occurrence,  $P_{\text{after}}/P_{\text{before}}$ , for the fully connected 45-mm pitch mesh is 42% and 52% for the strong and weak walls, respectively. This shows that the effect of the PP-band mesh increases as the masonry wall strength decreases.

Figure 19 depicts the deformed shapes of weak walls retrofitted with PP-bands. The finer and fully connected mesh is more effective to prevent the sliding of the upper wall portion and to distribute the diagonal cracking through a wider wall region. In terms of distributing the cracks, the 90-mm fully connected pitch performs better than the 45-mm partially connected pitch.

## CONCLUSIONS

A new technique for strengthening masonry structures is proposed. The method consists of using polypropylene bands (PP-bands), commonly used for packing, arranged in a mesh fashion and embedded in a mortar overlay. These bands are inexpensive, resistant, durable, and worldwide available. The effectiveness of the proposed retrofit is discussed from both experimental and numerical points of view.

The experiments showed that although the reinforcement did not increase the structure peak strength, it contributed to improve its performance after the crack occurrence. The reinforced walls exhibited larger post-peak strength and sustained their strength for lateral drifts larger than 2.0%. The mesh helped distributing the diagonal cracks over a wide region. The importance of the connectors and the mortar overlay for the retrofitted wall performance was recognized.

In order to discuss the effect of the mesh pitch, connection level, and wall strength, numerical simulations were carried out. It was found that coarser meshes adequately connected may perform as well as finer meshes partially anchored. This underscores the importance of the mortar overlay, which if adequately installed, provides connection between the mesh and the masonry wall. The beneficial effects of the PP-band mesh were clearer for weaker than for stronger walls.

Although several methods have already been proposed for masonry wall retrofitting, the use of PP-band meshes represents an inexpensive and easy to implement alternative. Other methods such as ferrocement coatings or FRP laminates effectively increase the structure strength. However, they present drawbacks such as corrosion risk, high costs and specialized labour for installation. To this end, the effect of the PP-band meshes for masonry wall retrofitting has only been tested under in-plane loads. Their effect on the out-of-plane behavior, efficiency to prevent wall corner cracking and separation, and effect on real dwellings subjected to dynamic motions still requires further investigation.

## REFERENCES

1. Houben H. and Guillaud, H. "Earth construction – A comprehensive guide." London: ITDG Publishing, 1989.
2. Coburn A. and Spence R. "Earthquake Protection." West Sussex: John Wiley & Sons Ltd, 1992.
3. Lizundia, B., Holmes, W. T., Longstreth, M., Kren, A., Abrams, D. P. "Development of Procedures to Enhance the Performance of Rehabilitated URM Buildings." NIST GCR 97-724-1, 1997.
4. Mayorca, P. "Strengthening of unreinforced masonry structures in earthquake-prone regions." University of Tokyo: PhD Dissertation, 2003.
5. Tagel-Din H. and Meguro K. "Applied Element Method for simulation of nonlinear materials: theory and application for RC structures." Struct. Engrg./Earthquake Engrg. 2000, 17(2), 137s-148s.
6. Pluijijm, R. Van Der. "Material properties of masonry and its components under tension and shear." Proc. 6<sup>th</sup> Canadian Masonry Symposium, Canada, 675-686, 1992.

7. Pluijim, R. Van Der. "Shear behavior of bed joints." Proc. 6<sup>th</sup> North American Masonry Conf., Philadelphia, 125-136, 1993.
8. Moreira Peñate, R. A. and Roales Inestroza, J. A. "Design, construction and quality control of adobe structures for rural housing." Centroamerican University "José Simeón Cañas": Undergraduate Thesis, 1998 (in Spanish.)